AFRL-DE-PS-TR-
2004-1050

DESIGN AND MEASUREMENT OF COBRA LENS ANTENNA PROTOTYPES FOR HPM EFFECTS TESTING APPLICATIONS

Clifton C. Courtney et al.

Voss Scientific
418 Washington St SE
Albuquerque, NM 87108

April 2004

Interim Report

AIR FORCE RESEARCH LABORATORY
Directed Energy Directorate
3550 Aberdeen Ave SE
AIR FORCE MATERIEL COMMAND
KIRTLAND AIR FORCE BASE, NM 87117-5776

STINFO COPY

AFRL-DE-PS-TR-2004-1050

This report has been approved for publication.

//signed//
ANDREW D. GREENWOOD, DR-III
Project Manager

//signed//
REBECCA N. SEEGER, Col, USAF
Chief, High Power Microwave Division

//signed//
L. BRUCE SIMPSON, SES
Director, Directed Energy Directorate

REPORT DOCUMENTATION PAGE

Form Approved
OMB No. 0704-0188

1. REPORT DATE *(DD-MM-YYYY)*	2. REPORT TYPE	3. DATES COVERED *(From - To)*
01-04-2004	Interim Report	01-03-2004 to 31-03-2004

4. TITLE AND SUBTITLE
Design and Measurement of COBRA Lens Antenna Prototypes for HPM Effects Testing Applications

5a. CONTRACT NUMBER
F29601-03-M-0101

5b. GRANT NUMBER

5c. PROGRAM ELEMENT NUMBER
65502F

6. AUTHOR(S)
Clifton C. Courtney, Tom McVeety, Jim Tate, and Donald E. Voss

5d. PROJECT NUMBER
3005

5e. TASK NUMBER
DP

5f. WORK UNIT NUMBER
CE

7. PERFORMING ORGANIZATION NAME(S) AND ADDRESS(ES)

Voss Scientific
418 Washington St SE
Albuquerque, NM 87108

8. PERFORMING ORGANIZATION REPORT NUMBER

9. SPONSORING / MONITORING AGENCY NAME(S) AND ADDRESS(ES)
AFRL/DEHE
3550 Aberdeen Ave SE
Kirtland AFB, NM 87117-5776

10. SPONSOR/MONITOR'S ACRONYM(S)

11. SPONSOR/MONITOR'S REPORT NUMBER(S)
AFRL-DE-PS-TR-2004-1050

12. DISTRIBUTION / AVAILABILITY STATEMENT
Approved for public release; distribution is unlimited.

13. SUPPLEMENTARY NOTES

14. ABSTRACT

For high power microwave susceptibility effects testing there is considerable interest in antennas that are high power capable, HPM source compatible and which radiate a broad, circularly polarized main beam. We have shown previously that the Coaxial Beam-Rotating Antenna (COBRA) Lens exhibits these properties, in theory. The COBRA Lens antenna transforms an azimuthally symmetric aperture field distribution, of the type common to many HPM sources, to a form that produces a centrally peaked radiation pattern with linear or circular polarization. The large aperture allows it to accommodate high power. The design, numerical simulation, and for the first time the measurement of two COBRA Lens antenna prototypes are summarized in this note. The resulting radiated patterns exhibit moderate directivity that makes them ideal for susceptibility testing applications where wide area coverage is desired. Finally, a brief discussion of the value of HPM susceptibility with circular polarization is provided.

15. SUBJECT TERMS
Electromagnetics; high power microwaves; antennas

16. SECURITY CLASSIFICATION OF:			17. LIMITATION OF ABSTRACT	18. NUMBER OF PAGES	19a. NAME OF RESPONSIBLE PERSON
a. REPORT	b. ABSTRACT	c. THIS PAGE			Andrew Greenwood
Unclassified	Unclassified	Unclassified	Unlimited	26	19b. TELEPHONE NUMBER *(include area code)* 505-846-6642

Standard Form 298 (Rev. 8-98)
Prescribed by ANSI Std. 239.18

Contents

List of Figures

1 Summary

For high-power-microwave susceptibility effects testing, there is considerable interest in antennas that are high-power capable, HPM-source compatible and which radiate a broad, circularly polarized main beam. We have shown previously that the Coaxial Beam-Rotating Antenna (COBRA) Lens exhibits these properties, in theory. The COBRA Lens antenna transforms an azimuthally symmetric aperture field distribution, of the type common to many HPM sources, into a form that produces a centrally peaked radiation pattern with linear or circular polarization. The large aperture allows it to accommodate high power. The design, numerical simulation and, for the first time, the measurement of two COBRA Lens antenna prototypes are summarized in this note. The first section reviews the design principles associated with the COBRA lens concept. Next, specific COBRA lens designs are formulated, and the results of finite-difference time domain (FDTD) numerical simulations of the response of COBRA lens designs are reported. Then, the measured patterns of the conical horn with no lens, with an N = 2 COBRA lens and with an N = 3 COBRA lens fitted to its aperture are provided. Next, comparisons of the measured and simulation results are made. The COBRA Lens prototype antennas are shown to produce linear or circular polarization on boresight, depending upon the lens fitted in the aperture of the conical horn. Furthermore, the resulting radiated patterns exhibit moderate directivity that makes them ideal for susceptibility testing applications where wide area coverage is desired. Finally, a brief discussion of the value of HPM susceptibility with circular polarization is provided.

2. Introduction

For high-power-microwave susceptibility effects testing, there is considerable interest in antennas that are high-power capable and which radiate a circularly polarized main beam. These attributes can be difficult to realize simultaneously, but we have shown previously that the Coaxial Beam-Rotating Antenna (COBRA) has these properties [Ref. 1, 3]. Furthermore, we have theoretically shown that a variant, the COBRA Lens antenna, behaves in a like manner and can be realized in a compact geometry [Ref. 2, 4]. The COBRA Lens antenna transforms an azimuthally symmetric aperture field distribution into a form that produces a centrally peaked radiation pattern with linear or circular polarization. The design, numerical simulation and measurement of a COBRA lenses are summarized in this note. The first section reviews the design principles associated with the COBRA lens concept. Next, specific lens designs are formulated, and the results of finite-difference time domain (FDTD) numerical simulations of the response of COBRA lens designs are reported. Then, the measured patterns of the conical horn with no lens, with an N = 2 COBRA lens, and with an N = 3 COBRA lens fitted to its aperture are provided. Next, comparisons of the measured and simulation results are made. Finally, a brief discussion of the value of HPM susceptibility with circular polarization is provided.

3. COBRA Lens Antenna Design

In this section a description for general design of a COBRA Lens antenna is reviewed. Then, the specific designs are conducted for the conical horn, and the N = 2 and N = 3 COBRA lenses.

3.1 General COBRA Lens Design Equations

The general design of a COBRA lens is dictated by the need to advance or retard the phase of the aperture field by a prescribed amount [Ref. 2, 4]. To do so, the lens geometry is defined simply by the requirement that the optical path length is altered, by adding additional dielectric material, in a prescribed manner. Specifically, the phase difference between lens sectors is given by

$$\Delta\varphi = \frac{2\pi(n-1)}{N} \qquad \text{for } n = 1, 2, \ldots, N. \tag{1}$$

where N=number of steps in the lens surface. For this phase difference to be accomplished, the sector step size must be given by the following

$$\Delta\varphi = \frac{2\pi(n-1)}{N} = \beta l\sqrt{\varepsilon_r} - \beta l = \beta l(\sqrt{\varepsilon_r} - 1). \tag{2}$$

The step size is then

$$\Delta l = \frac{1}{N}\frac{\lambda}{\sqrt{\varepsilon_r} - 1}, \tag{3}$$

and the thickness of each sector is

$$l_n = \frac{2\pi(n-1)}{N}\frac{1}{\beta(\sqrt{\varepsilon_r} - 1)} = \frac{(n-1)}{N}\frac{\lambda}{\sqrt{\varepsilon_r} - 1}, \qquad \text{for } n = 1, 2, \ldots, N. \tag{4}$$

3.2 Conical Horn Design

For the design of these COBRA Lens antenna prototypes, the nominal frequency of 3 GHz (l_0=4.01 inches) was chosen. Consequently, the diameter of the circular waveguide that feeds the conical horn was chosen to be 3.36 inches; this gives a TM_{01} mode cutoff frequency of f_c=2.689 GHz and a guide wavelength for this mode of λ_g = 8.88 inches.

The conical horn flares from the circular waveguide radius of 3.36 inch diameter to its final aperture diameter of 16 inches over a 16 inch axial length. The TM_{01} mode wavelength at this diameter is l_g = 4.01 inches. As the horn reaches this final diameter, there is an extent of straight circular guide. The purpose of this straight length of guide is to hold the COBRA lens;

its length depends on whether the N = 2 (3.88 inches) or N = 3 (5.17 inches) lens is held in the aperture. The geometry and dimensions of the conical horn are indicated in Figure 1.

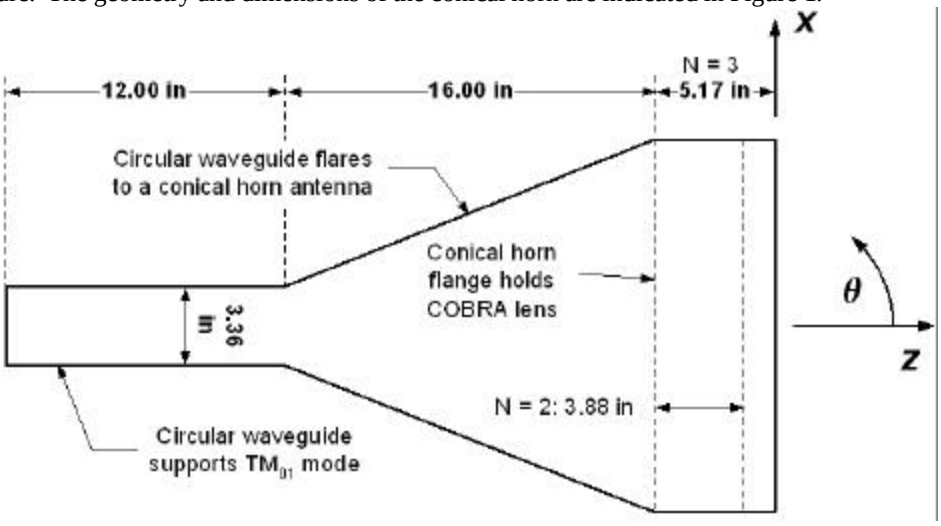

(a)

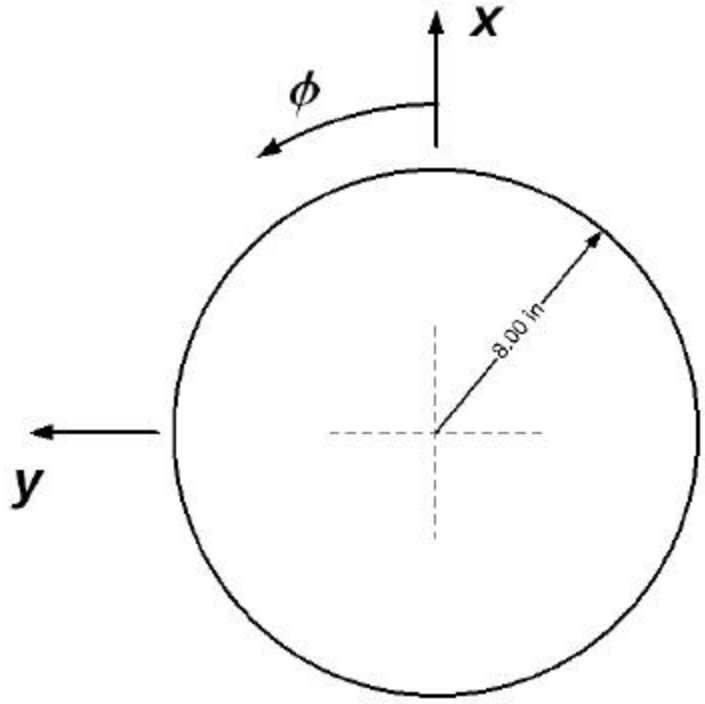

(b)

Figure 1. Geometry of the 16 inch diameter conical aperture antenna: (a) xz-plane; and (b) xy-plane.

The aperture area of the conical horn is

$$A = \pi r^2 = \pi \times (8)^2 = 201.06 \text{ in}^2 = 1{,}297.17 \text{ cm}^2.$$

Consequently, the aperture gain is

$$G_A = \frac{4\pi}{\lambda^2} Area = \frac{4\pi}{(3.94)^2} \times 201.06 = 162.75$$

numerical and 22.11 dB. The power capacity of the aperture can be estimated as

$$P = Area \times 1 \frac{MW}{cm^2} \times \alpha = 1{,}297.17 cm^2 \times 1 \frac{MW}{cm^2} \times \alpha = 1{,}297.17 \times \alpha \text{ MW}$$

where 1 MW/cm^2 is the typical air breakdown limit and α is a safety de-rating factor. Letting $\alpha = 0.25$, then, gives a power capacity for the 16 inch diameter circular aperture of ~ 325 MW.

3.3 N = 2 COBRA Lens Design

The geometry of the N = 2 COBRA lens is simply half of a right circular cylinder bisected along its longitudinal axis. From above, the height of the cylinder, or thickness of the lens, is

$$\Delta l = \frac{1}{2} \frac{\lambda_g}{\sqrt{\varepsilon_r} - 1}$$

High density polyethylene (HDPE) is chosen as the lens material, with $\varepsilon_r = 2.3$; then

$$\Delta l = \frac{1}{2} \frac{4.01}{\sqrt{2.3} - 1} = 3.88 \text{ inch.}$$

The geometry of the N = 2 COBRA lens design is shown in Figure 2.

3.4 N = 3 COBRA Lens Design

From earlier work, we know that an N = 3 COBRA lens is required to produce circular polarization on boresight [Ref. 1, 2]. The geometry of the N = 3 COBRA lens is more complicated than that of the N = 2 lens and not easily categorized. However, from above, the thicknesses of each sector of the lens are given by:

$$l_1 = \frac{(1-1)}{3} \frac{\lambda_g}{\sqrt{\varepsilon_r} - 1} = 0,$$

$$l_2 = \frac{(2-1)}{3} \frac{\lambda_g}{\sqrt{\varepsilon_r} - 1} = \frac{1}{3} \frac{4.01}{\sqrt{2.3} - 1} = 2.59 \text{ inches, and}$$

$$l_3 = \frac{(3-1)}{3} \frac{\lambda_g}{\sqrt{\varepsilon_r} - 1} = \frac{2}{3} \frac{4.01}{\sqrt{2.3} - 1} = 5.17 \text{ inches.}$$

Again, HDPE is chosen as the lens material, with $\varepsilon_r = 2.3$. The geometry of the N = 3 COBRA lens design is shown in Figure 3.

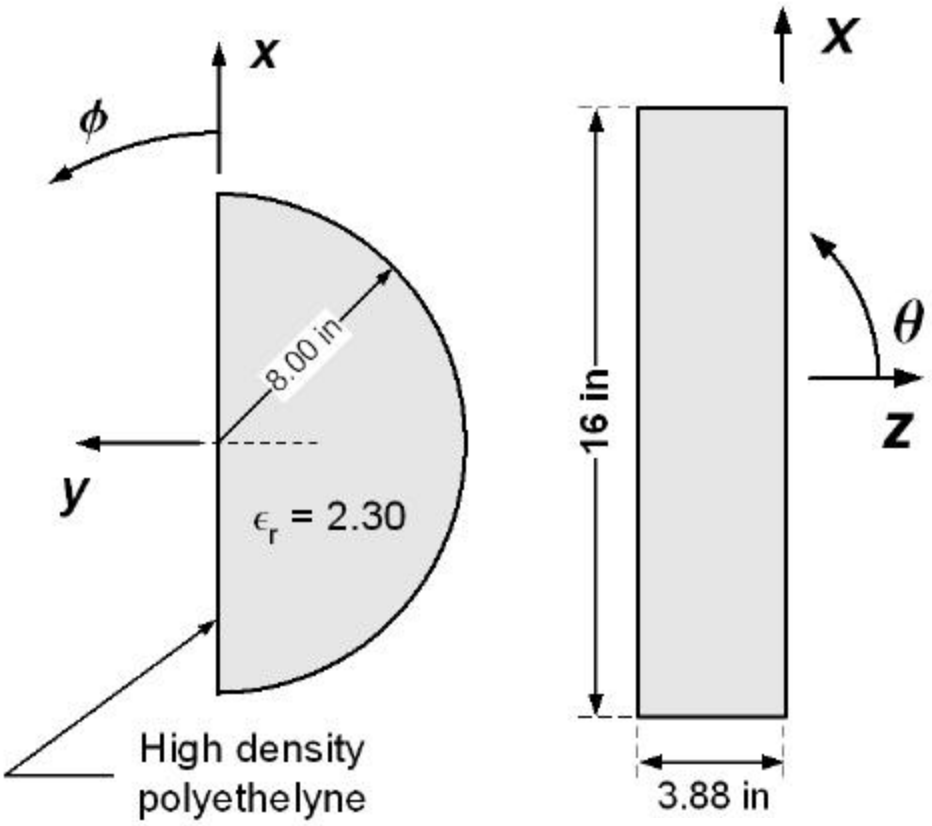

Figure 2. Geometry of the 16 inch diameter, N = 2 COBRA lens made from high density polyethylene (e_r = 2.30): (a) xz-plane; and (b) xy-plane.

4. FDTD Simulation of COBRA Lens Antenna Designs

The geometry of the COBRA Lens antenna designs described above were rendered as finite difference grids with a cubic grid size of less than 0.125 inches. Electromagnetic simulations of the geometries were then conducted and the steady state radiated patterns computed. The computational results for each geometry described above are presented below.

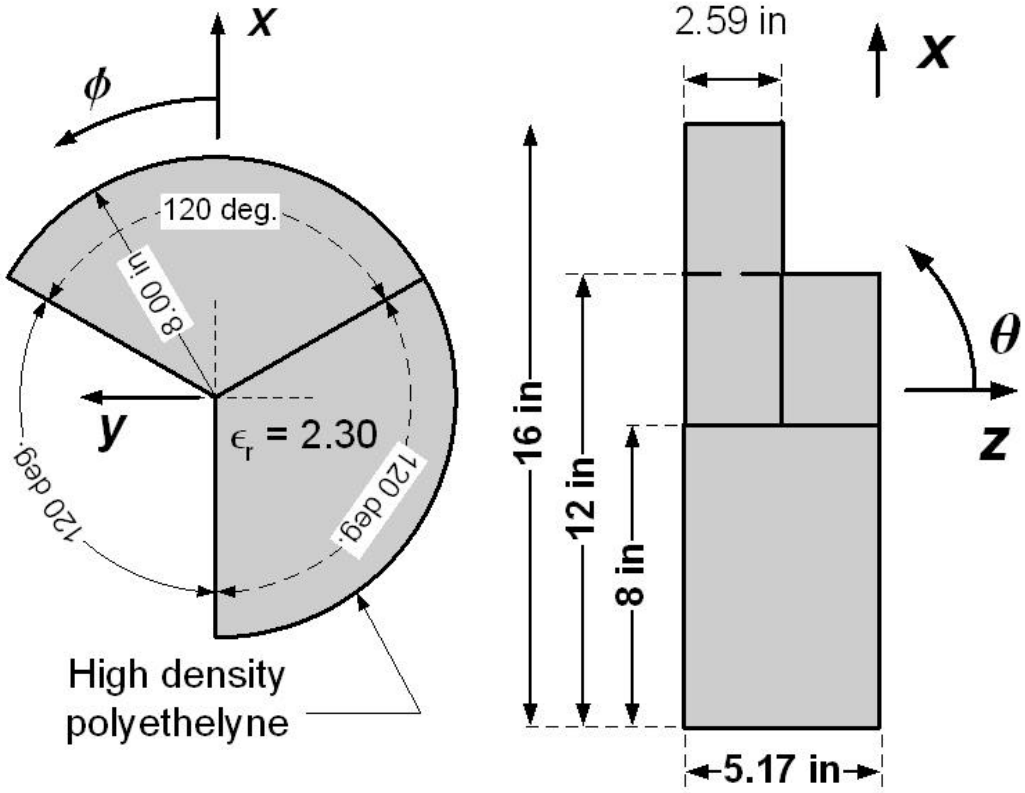

(a) (b)

Figure 3. Geometry of the 16 inch diameter, N = 3 COBRA lens made from high density polyethylene (e_r = 2.30): (a) xz-plane; and (b) xy-plane

4.1 FDTD Simulation of Conical Horn Antenna

A TM_{01} mode was established in the 3.36 inch diameter section of the circular waveguide feed by driving a centered wire against the back plate of the guide. The resulting azimuthally symmetric mode radiates a single dominant polarization pattern with a null on boresight. The computed pattern of the conical horn antenna is shown in Figure 4. For this case, there was no straight section of guide (see included geometry in graph). The peak gain of the pattern is seen to be ~ 14.5 dB.

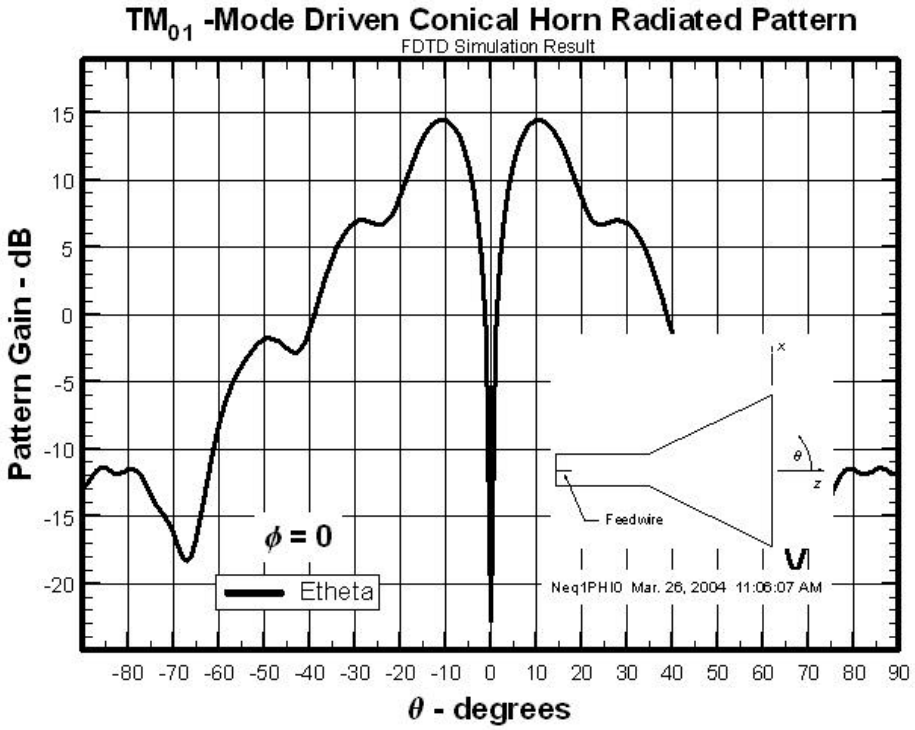

Figure 4. The radiated pattern of a TM01-mode driven, 16 inch diameter, circular aperture, conical horn antenna as computed by FDTD simulation at 3 GHz.

4.2 FDTD Simulation of N = 2 COBRA Lens Antenna

Next, the N = 2 COBRA Lens and the straight section to hold it was added to the finite difference geometry. As described above, the lens was HDPE with a relative permittivity of ε_r = 2.3. The azimuthally symmetric waveguide mode was established in the same way and the resulting radiated pattern was computed. In this case, the lens / air interface in the aperture was along the *x*-axis. The radiated patterns of the dominant polarizations in the principal planes of an N = 2 COBRA Lens antenna are shown in Figure 5. One notes that although the radiated pattern exhibits linear polarization and a boresight peak, the patterns differ along the two principal planes. The peak gain of the pattern is seen to be ~ 16.6 dB.

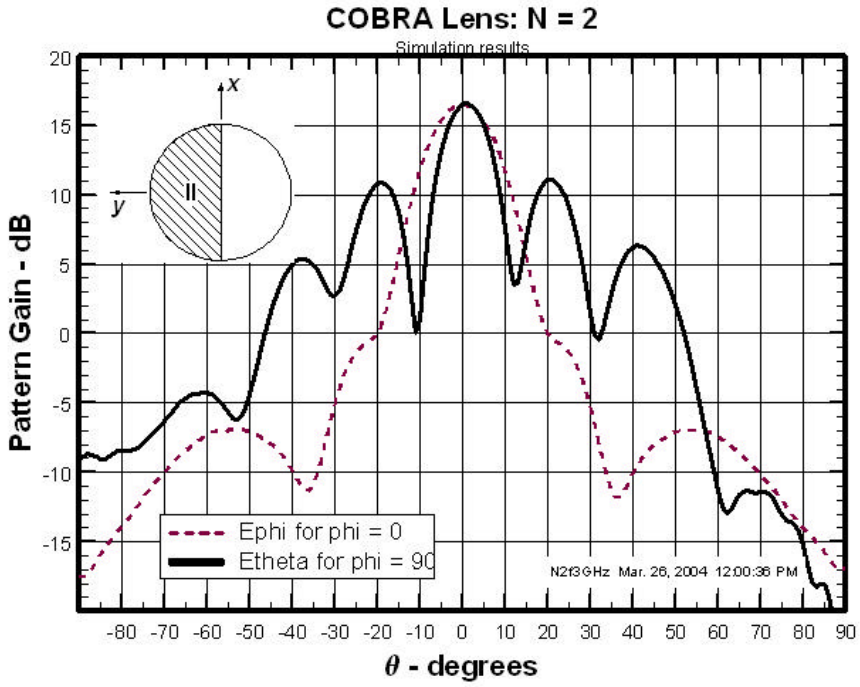

Figure 5. The radiated patterns of the dominant polarizations in the principal planes of an N = 2 COBRA Lens antenna.

4.3 FDTD Simulation of N = 3 COBRA Lens Antenna

Finally, the N = 3 COBRA Lens and its associated straight section to hold it was added to the finite difference geometry. The radiated patterns of the dominant polarizations in the principal planes of an N = 3 COBRA Lens antenna are shown in Figure 6. The boresight ($\theta = 0$) gain for each polarization was 12.4 dB. The phase difference between the orthogonal polarizations on boresight was either 98.5 degrees, or 81.5 degrees depending on which principal plane was examined. Nonetheless, the difference from 90 degrees between the two polarizations was 8.5 degrees in each case. Consequently, the boresight field is circularly polarized, to a high degree of fidelity.

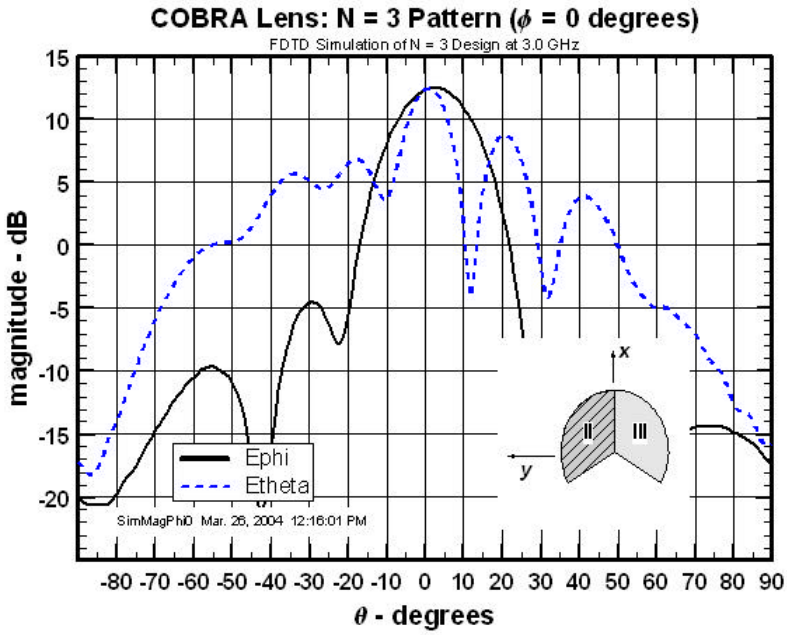

(a)

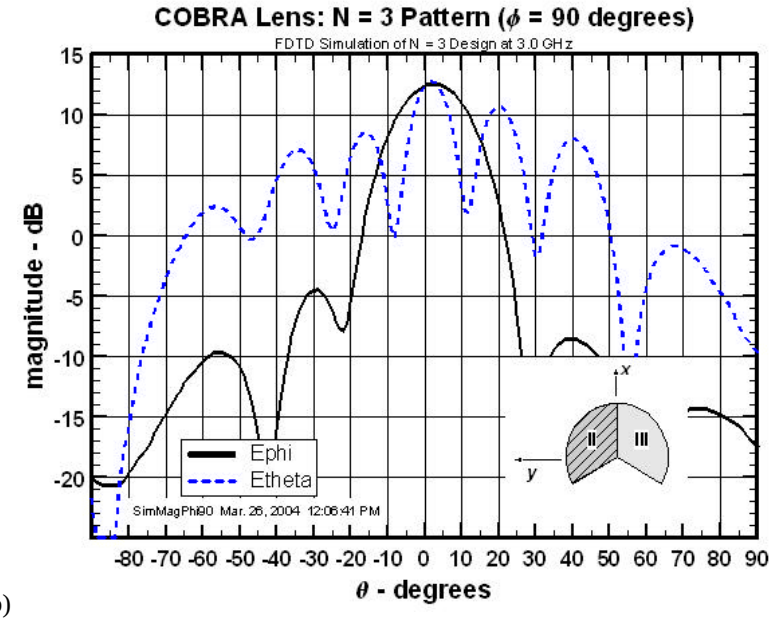

(b)

Figure 6. The radiated patterns of each polarization in the principal planes of an N = 3 COBRA Lens antenna: (a) f = 0 degrees; and (b) f= 90 degrees.

5. Fabrication of COBRA Lens Antenna Prototypes

The prototype antenna designs described in this report were implemented in hardware. Three piece parts that together constituted the conical horn and lens holding assemblies were fabricated from aluminum. The lenses were made from high density polyethylene. CAD renderings of the N = 2 and N = 3 COBRA Lens antennas are shown in Figure 7. Note that the straight sections that accept and support the COBRA lenses have flanges on each side and are attached to the conical horn through an array of bolts. This allows the same conical horn to be used in both antenna prototypes. Photographs of the piece parts for the two antennas are shown in Figure 8, while the assembled N = 3 COBRA Lens antenna is shown in Figure 9. An SMA feed through connector was inserted through the center of the rear wall of the circular waveguide; its geometry possessed the necessary symmetry to preferentially stimulate the TM_{01} circular waveguide mode. An additional length of wire was added to the connector's inner conductor for tuning; the resulting feed exhibited greater than 25 dB of return loss at the design frequency.

(a)

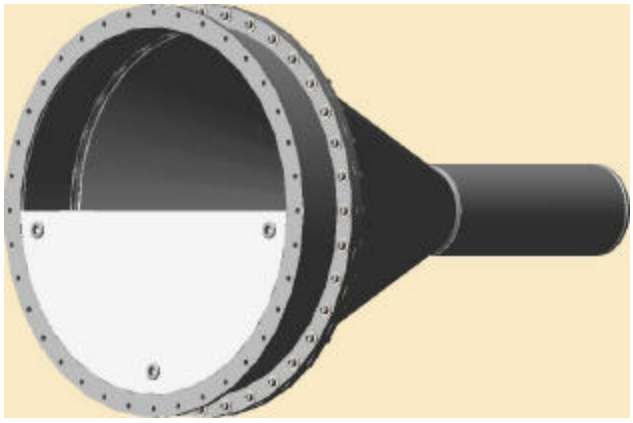

(b)

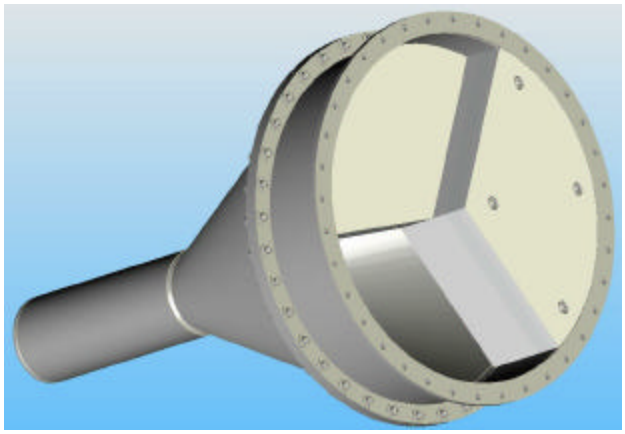

Figure 7. CAD renderings of COBRA Lens Antenna designs: (a) N = 2; and (b) N = 3.

(a)

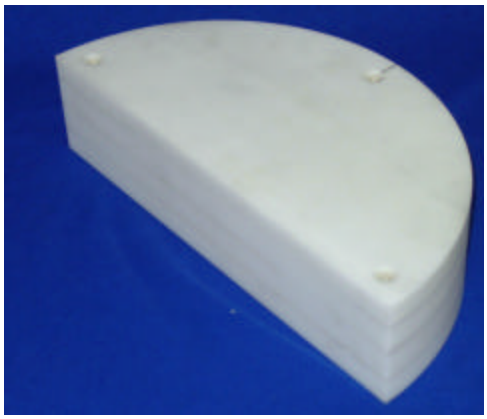

(b)

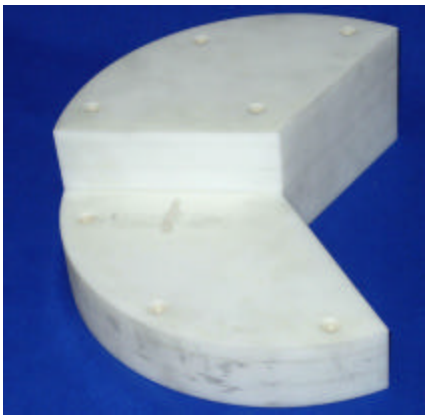

(c)

Figure 8. **Piece parts of the COBRA Lens antenna prototype: (a) conical horn with N = 2 and N = 3 lens attachment fixtures, all made of aluminum; (b) N = 2 lens made of HDPE; and (c) N = 3 lens also made of HDPE.**

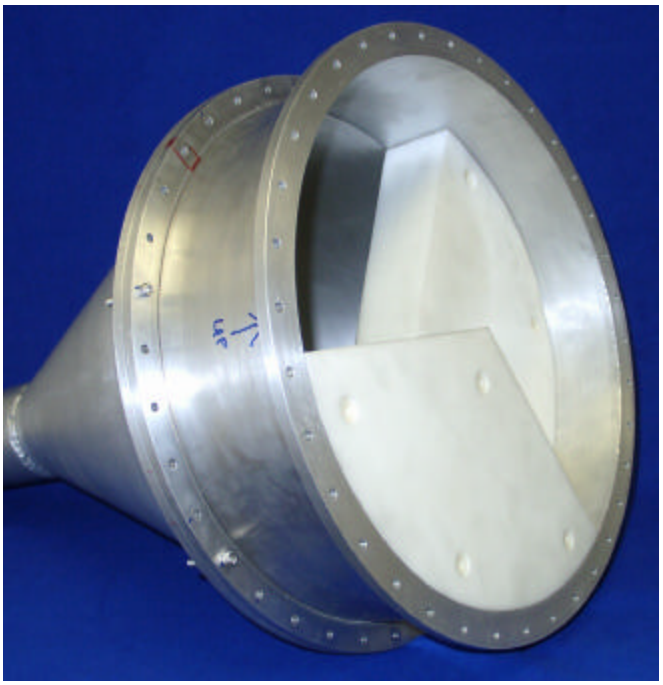

Figure 9. Photograph of the COBRA Lens N = 3 prototype antenna.

6. Measurement of COBRA Lens Antennas

Extensive measurements of the radiated pattern of the N = 2 and N = 3 COBRA Lens antenna prototype antennas were made. These measurements were conducted under somewhat non-ideal conditions in an open field adjoining the Voss Scientific offices. The COBRA Lens antennas were placed atop an azimuthal positioner and configured as the transmit antenna, while a cutoff WR-284 open ended waveguide was made the receive antenna. A metal-sided, Morgan building was located about six feet behind the transmit antenna, and the close proximity to the rear of the antenna probably reduced our ability to measure sidelobes accurately.

Figure 10. Pattern measurement configuration.

6.1 Measurement of N = 2 COBRA Lens Antenna

The measured patterns of the dominant polarizations of the N = 2 COBRA Lens antenna in its principal planes are shown in Figure 11. Note that the pattern cut that goes along the COBRA lens interface has a broad main lobe and low side lobes. The pattern cut that goes across the interface gives a narrower main lobe with higher side lobes.

6.2 Measurement of N = 3 COBRA Lens Antenna

The measured patterns of the dominant polarizations of the N = 3 COBRA Lens antenna in its principal planes are shown in Figure 12. Note that on boresight the gain of the two polarizations differs by < 1 dB.

Shown in Figure 13 are the values of measured boresight gain as a function of frequency for the two orthogonal polarizations radiated by the N = 3 COBRA Lens antenna. Also shown in the graph is the magnitude of the difference between the two curves. One notes that at the design frequency of 3 GHz, the gain difference is ~ 1 dB. Shown in Figure 14 is the measured phase of each polarization, measured for the boresight position, as a function of frequency. Also indicated on the graph is the difference between the measured values of phase. One notes that the phase difference at the design frequency is ~ 81 degrees.

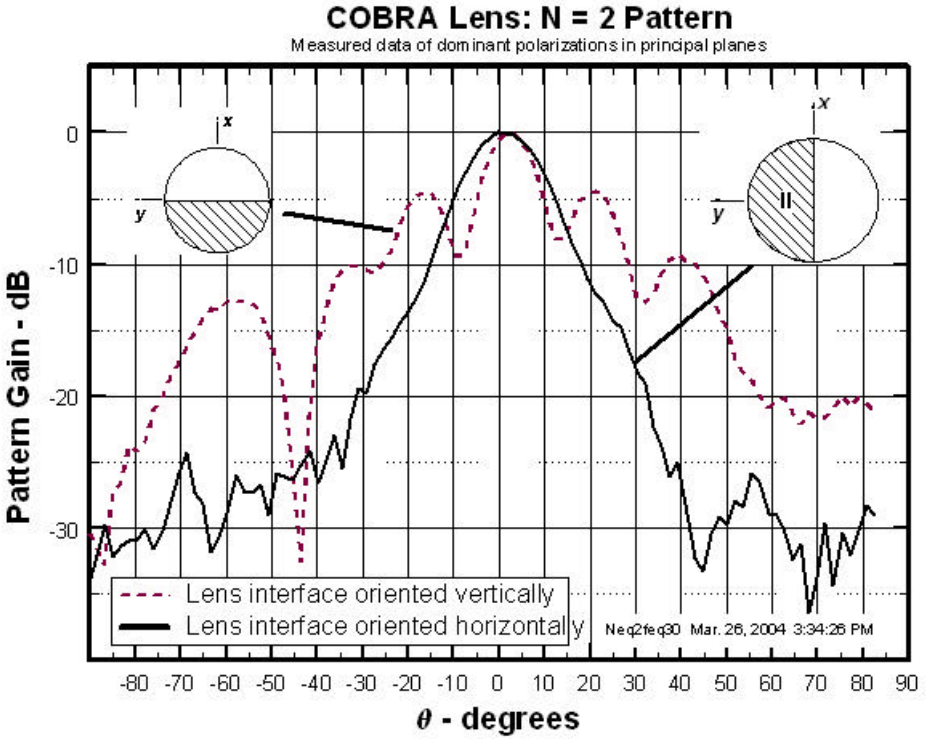

Figure 11. The measured patterns of the dominant polarizations of the N = 2 COBRA Lens antenna in its principal planes.

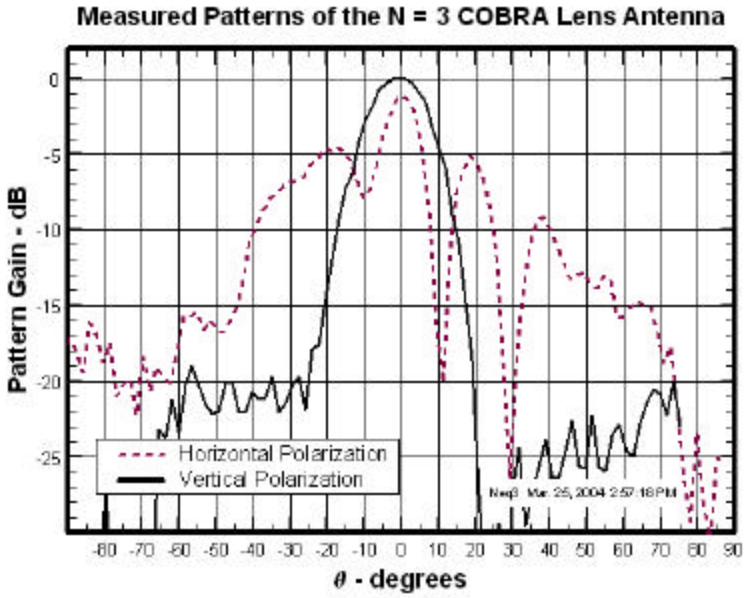

Figure 12. Measured patterns of two polarizations of the N = 3 COBRA Lens antenna.

7. Comparison of Measured and Simulated Properties of COBRA Lens Antennas

In this section, comparisons of the measured and computed radiated patterns of N = 2 and N = 3 COBRA Lens antennas are made. These results are taken directly from the results reported in previous sections on measured and computed patterns of the COBRA Lens antennas; they have simply been presented together in the same graphs.

7.1 Comparison of N = 2 COBRA Lens Antenna Results

For the N = 2 COBRA Lens antenna, the radiated pattern should exhibit linear polarization with a peak on boresight. In Figure 14, comparisons of calculated and measured radiated patterns of the N = 2 COBRA Lens Antenna are shown; in (a) a graph of the lens oriented horizontally to the y-axis is shown; while in (b) the lens is oriented vertically. The values of gain have been adjusted in the measured data to allow direct comparison with the computed values. Good agreement is noted in the main beam of radiated patterns in both principal planes.

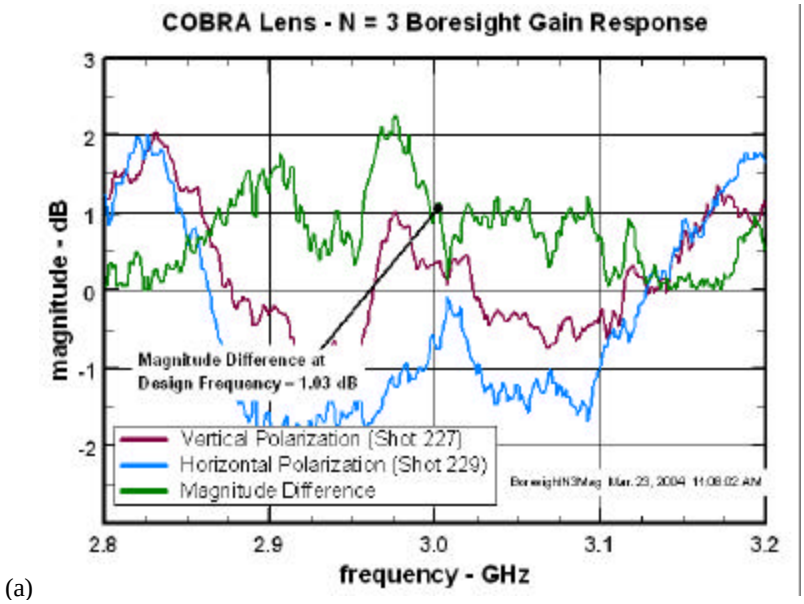

(a)

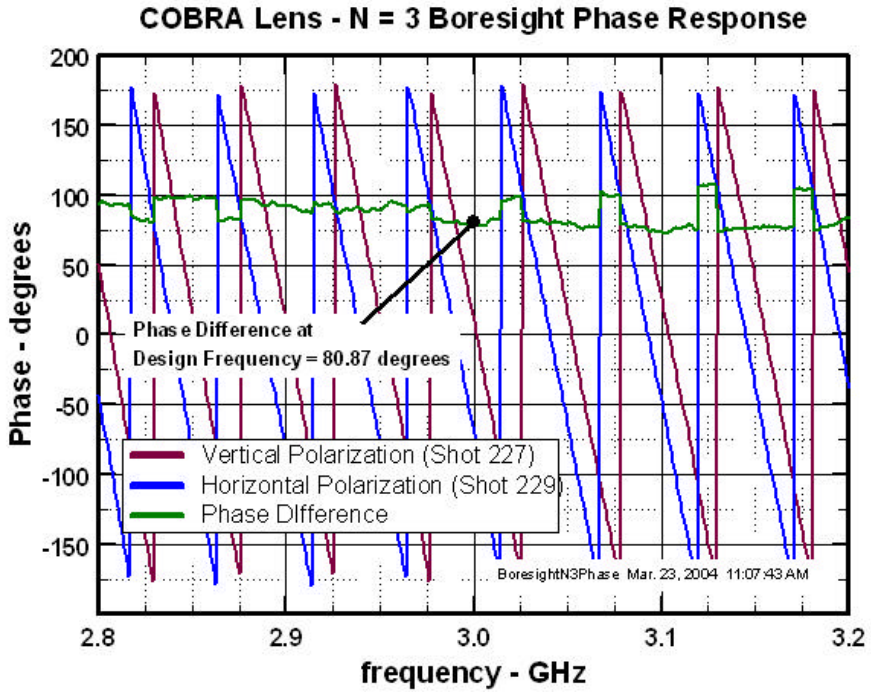

(b)

Figure 13. The measured boresight properties of the N = 3 COBRA Lens antenna at the design frequency = 3 GHz: (a) magnitude; and (b) phase.

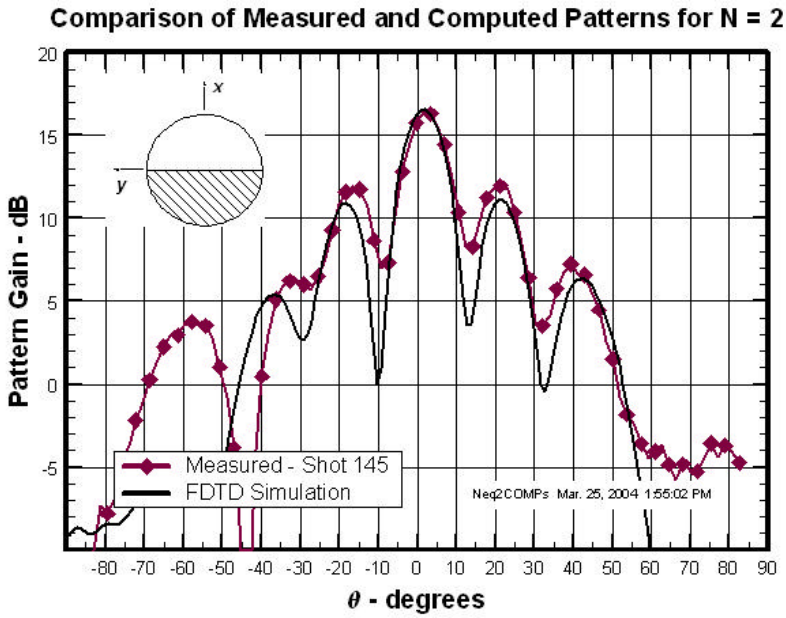

(a)

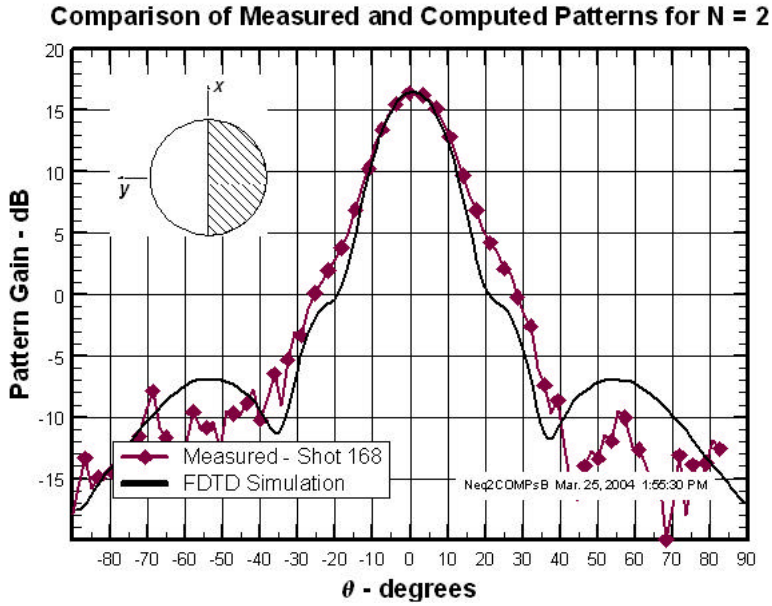

(b)

Figure 14. Comparison of calculated and measured radiated patterns of the N = 2 COBRA Lens Antenna: (a) lens oriented horizontally; and (b) lens oriented vertically.

7.2 Comparison of N = 3 COBRA Lens Antenna Results

For the N = 3 COBRA Lens antenna, the radiated pattern should exhibit circular polarization, with a peak on boresight. In Figure 15, comparisons of calculated and measured radiated patterns of the N = 3 COBRA Lens Antenna are shown; in (a) a graph of the pattern of the vertically polarized component is shown; while in (b) is a graph of the radiated pattern of the horizontally polarized component. Again, the values of gain have been adjusted in the measured data to allow direct comparison with the computed values. Good agreement is noted in the main beam of radiated patterns.

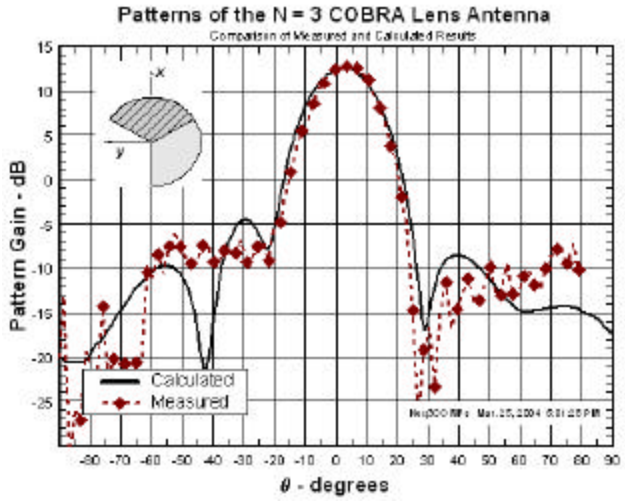

(a)

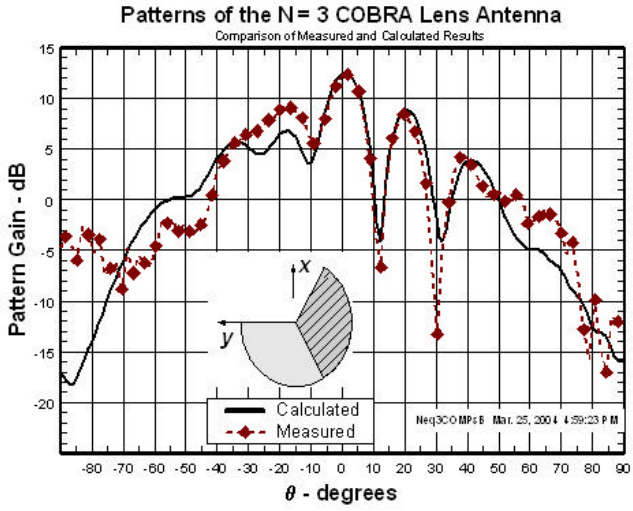

(b)

Figure 15. Comparison of calculated and measured radiated patterns of the N = 3 COBRA Lens Antenna: (a) vertical polarization; and (b) horizontal polarization.

8. Conclusion

In this paper, we have presented the design of two, S-band COBRA Lens antennas. The N = 2 COBRA Lens produces linear polarization on boresight, while the N = 3 COBRA Lens antenna generates circular polarization on boresight. The results of extensive finite difference simulations of these designs were also given. These results validated the design and performance of each antenna prototype. In addition, for the first time, we have fabricated two prototype antennas and measured their radiating properties. Experimental data associated with these measurements have been formatted and are furnished in this paper. The experimental results validate the expected performance of the N = 2 and N = 3 COBRA Lens prototype antennas. Finally, comparisons were made of the computed and measured antenna characteristics of both prototype antennas. Good agreement was noted for all cases.

In conclusion, we have computationally and experimentally validated the performance of the COBRA Lens antenna concepts. The performance of the COBRA Lens antenna makes it a strong candidate for HPM effects testing applications. It is: (1) compatible with the output mode of many HPM sources; (2) requires no mode converter; (3) generates linear or circular polarization on boresight; and produces a broad main beam that is ideal for maximizing the HPM field coverage area and minimizing the separation distance between the antenna and the test zone. HPM effects testing with circular polarization is the preferred method of susceptibility testing since it excites and maximizes the coupling through arbitrarily oriented apertures. In principle, testing with circular polarization could reduce the amount of testing required, since both polarizations are present simultaneously. This effectively reduces by half the number of test configurations required. Finally, circular polarization could enhance HPM effects if multiple coupling paths, each with an arbitrary orientation, contribute to the total electromagnetic field within an enclosure.

REFERENCES

1. "Coaxial Beam-Rotating Antenna (COBRA) Concepts," C. Courtney and C. E. Baum, AFRL Sensor and Simulation Note 395, April 1996.
2. "Design and Numerical Simulation of the Response of a Coaxial Beam-Rotating Antenna Lens," C. Courtney, et al., AFRL Sensor and Simulation Note 449, August 2000.
3. "The coaxial beam-rotating antenna (COBRA): theory of operation and measured performance," C. Courtney and C. E. Baum, IEEE Trans. on Antenna and Propagation, vol. 48, no. 2, Feb., 2000.
4. "Design and Numerical Simulation of a Coaxial Beam-Rotating Antenna Lens," Clifton Courtney, Electronic Letters, Institution of Electrical Engineers, United Kingdom, May 2002.

DISTRIBUTION LIST

DTIC/OCP 8725 John J. Kingman Rd, Suite 0944 Ft Belvoir, VA 22060-6218	1 cy
AFRL/VSIL Kirtland AFB, NM 87117-5776	2 cys
AFRL/VSIH Kirtland AFB, NM 87117-5776	1 cy
AFRL/DEHP/Dr. Thomas Spencer Kirtland AFB, NM 97117-5776	1 cy
AFRL/DEHP/Mr. Robert Torres Kirtland AFB, NM 97117-5776	1 cy
Voss Scientific 418 Washington St SE Albuquerque, NM 87108	4 cys
Official Record Copy AFRL/DEHE/Dr. Andrew Greenwood	2 cys